AIP | Review of Scientific Instruments

Terahertz antenna electronic chopper

L. A. Sterczewski, M. P. Grzelczak, and E. F. Plinski

Citation: Review of Scientific Instruments **87**, 014702 (2016); doi: 10.1063/1.4939461
View online: http://dx.doi.org/10.1063/1.4939461
View Table of Contents: http://scitation.aip.org/content/aip/journal/rsi/87/1?ver=pdfcov
Published by the AIP Publishing

Terahertz antenna electronic chopper

L. A. Sterczewski,[a] M. P. Grzelczak, and E. F. Plinski
Department of Electronics, Wroclaw University of Technology, 27 Wybrzeze Wyspianskiego St., 50-370 Wroclaw, Poland

(Received 18 May 2015; accepted 19 December 2015; published online 6 January 2016)

In this paper, we present an electronic circuit used to bias a photoconductive antenna that generates terahertz radiation. The working principles and the design process for the device are discussed in detail. The noise and shape of the wave measurements for a built device are considered. Furthermore, their impact on a terahertz pulse and its spectra is also examined. The proposed implementation is simple to build, robust and offers a real improvement over THz instrumentation due to the frequency tuning. Additionally, it provides for galvanic isolation and ESD protection. © *2016 AIP Publishing LLC.* [http://dx.doi.org/10.1063/1.4939461]

I. INTRODUCTION

Terahertz generation and measurements are very susceptible to noise, as the power generated by photoconductive antennas is in the order of magnitude of nanowatts.[1,2] A photoconductive antenna (PCA), in its simplest form, is a two-metal electrode deposited on a semi-insulating substrate with a gap between these two electrodes.[3] Energy is stored in the gap until the femtosecond pulse hits the spot acting as a switch. A laser pulse switches the reservoir of stored energy and releases it in the form of THz radiation.[4] Free carriers are driven by the bias field across the gap and produce photocurrent.

An optical chopper is often used to modulate the intensity of the laser pulses exciting the generation of terahertz waves to handle the measurement of a signal with noise greater than the useful signal. A modulated temporal waveform, after reception, can be extracted from the noise using a homodyne detection scheme.[5]

Lock-in measurements require a reference frequency. Commonly, the frequency remains constant over the course of the experiment (from an oscillator or function generator) and the lock-in amplifier (LIA) detects the response from the experiment at the reference frequency. Noise signals at frequencies different from the reference frequency are rejected and do not affect the measurement.

Typically, the signal-to-noise ratio of the THz pulse is strongly affected by the 1/f noise characteristics of the mode-locked laser and can be improved effectively by increasing the modulation frequency.[6] Researchers have however reported modulating the bias electric field applied to the PC antenna instead of modulating the intensity of the laser pulses that excite a PC antenna.[7] This fact led us to employ the electronic frequency-tunable chopper and to measure its noise characteristics over the frequency range from 32 up to 100 kHz.

II. THz MEASUREMENT SETUP

Roughly speaking, our time-domain spectrometer[8] consists of an ultrafast pulse laser source, two photoconductive antennas and the biasing circuit. The path of the infrared femtosecond laser is split into two beams which create the arms of the interferometer. A motorized variable delay line increases or decreases the optical path. It provides an opportunity to, in some way, scan the generated terahertz time impulse response. However, the time impulse can only be reconstructed, thanks to coherent detection.[9] The setup is shown in Fig. 1.

The excitation source was a mode-locked femtosecond erbium-doped fiber laser with a pulse width of the 82 fs and repetition rate of 100 MHz. The center laser wavelength was set to 780 nm. The output of the laser (divided into two beams, at a power ratio of 60%–40%) was guided and focused by an objective lens onto the PC antennas. It is favorable for the pump pulse's spot diameter to be approximately 1.2 of the gap of a dipole.[10] To achieve an activity condition, focusing lenses were employed. It was enough to symmetrically excite the PC antenna with laser pulses. The amplitude of the applied bias voltage was typically 20 V, ensuring operation far from the breakdown voltage threshold of the substrate.

The probing pulse's delay was realized by employing the retro-reflector corner cube mounted on the motorized linear line. It is controlled by composed software of the LabVIEW environment. The resolution of the stage is limited by steps per revolution of the stepper motor and was approximately 4 μm. The PC antenna itself is a 200 μm-long dipole with the 5 μm gap,[11] optimized for imaging and photomixer applications, with a maximum spectral peak located at around 0.2 THz. The structure is fabricated on a low-temperature-grown gallium arsenide. To collimate the terahertz waves, a hyper-hemispherical lens made out of the high-resistive silicon was used. At the critical emission angle equal to 90°, the output rays emerge at an angle equal to 17°, which is implied by the refractive index of the high-resistivity silicon. This design does not lead to spherical aberration and ensures the absence of total internal reflection.[12] Unlike standard mirrors, off-axis parabolic metal mirrors direct and focus an incident collimated light at a specific angle. The all-reflective arrangement eliminates the phase delays and absorption losses introduced by the transmissive optics.

The signal is processed by the lock-in amplifier in order to enhance the signal-to-noise ratio. It ought to be synchronized

[a]Electronic mail: lukasz.sterczewski@pwr.edu.pl

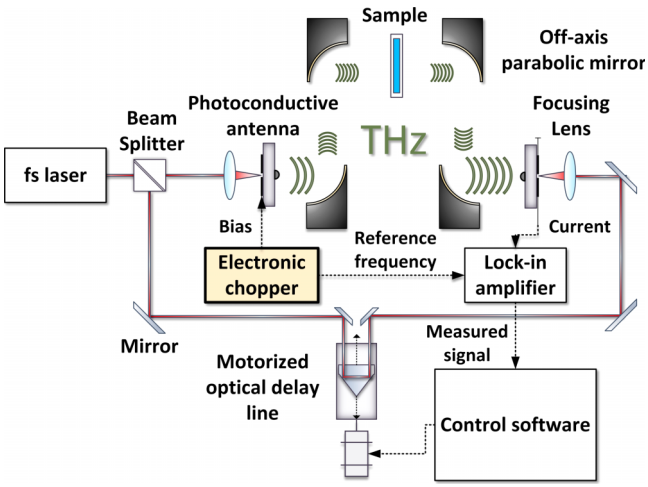

FIG. 1. Schematic block diagram of the THz measurement setup.

with the reference frequency, which is generated by an optical or electronic chopper. However, when an electronic chopper is used, it can effectively double the amplitude of the temporal waveform of the terahertz waves doubling the SNR.[13] Fig. 2 shows the differences in setup when electronic or optical chopper (300CD, Scitec Instruments, UK) is applied, respectively.

III. ELECTRONIC CHOPPER

Since traditional high-voltage modulators are linear amplifiers driving a step-up transformer, which operates up to 200 kHz, an enormous amount of power is being dissipated. Our circuit bypasses this issue by working in non-ohmic region of the MOSFET's characteristics. The terahertz photoconductive antenna can be biased with a bipolar square wave directly by a MOSFET H-Bridge,[14] yet it does not provide any galvanic isolation.[15] Moreover, such a driving scheme requires two symmetrical wires and the ground to be connected to the PC antenna. Instead of this, a separating transformer can be introduced. The main advantages of this are elimination of the unwanted common-ground coupling, and only two wires connecting the biasing circuit—the biasing and the ground. Additionally, a step-up transformer, instead of running at 1:1, can be easily wound to multiply the input voltage without the need to build a dedicated power supply. The schematic diagram is shown in Fig. 3.

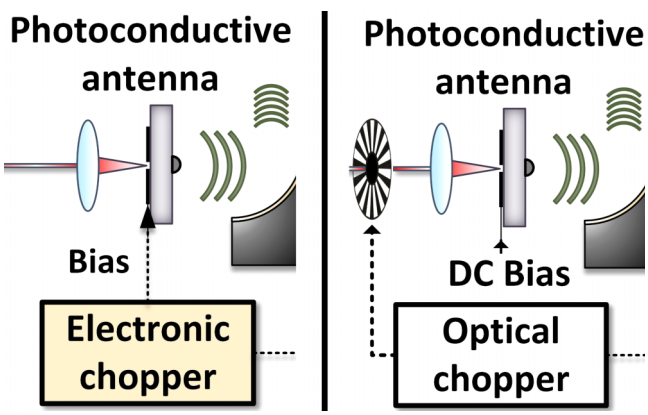

FIG. 2. Differences in setup.

A. MOSFET driver

The MOSFET switching time transitions can be reduced if driven by a high-speed, high-current totem-pole driver. A wide range of general purpose integrated circuits offer a peak output of 1.5 A, which ensures rise and fall times in the vicinity of 50 ns at a load of 1 nF.[16] The initial idea to keep the design as simple as possible prompted us to design our own gate driver circuit based on an NPN-PNP emitter follower. It consists of the CMOS Schmitt triggers working as buffers for the generator. A parallel connection boosts the bipolar transistor current. The counter phase commutation is provided by an additional negation, which also benefits from the introduced delay, of 80–200 ns for a 10 V power supply, which eliminates the cross-conduction action of the MOSFETs.

Taking into consideration that the FETs' capacitance and transformer's inductance form a resonant L/C tank, the snubber circuit[17] has to be used to diminish the oscillations. For critical damping ($\xi = 1$), the values of the snubbing components can be estimated from the given conditions: $C_{SNUB} \geq 5 \times C_S$ and $R_{SNUB} = 1/2 \times \sqrt{L_S/C_S}$, where C_S is a calculated effective capacitance at the switch node, the value of which is empirically derived by adding an external capacitor of a capacitance causing the ringing frequency to be lowered by half. The obtained value has to be divided by 3. L_S can be calculated from $1/(C_S \times (2\pi \times f_{RINGING})^2)$.

The proposed solution has a few drawbacks. Its peak gate drive current depends on the gain of the transistors. Transition times suffer from the slower PNP switching. It should be noticed that when a driven voltage on a gate of the power transistor exceeds the supply voltage, it can, eventually, cause the device to turn off. Nevertheless, experiments have shown that the unwanted effects mentioned above do not occur. The turn-on and turn-off times were measured to be roughly 90 ns. This is considered to be a good performance.[18]

B. Transformer design

The quadrifilar center-tapped push-pull toroidal transformer has been designed[19] and wound onto a 3E25 ferrite toroidal core, with the serial number TN25/15/10-3E25 (Ferroxcube). It is arranged in a voltage-doubling configuration with the secondary side center tap unconnected. The quadrifilar winding technique provides a high primary-to-secondary coupling, minimizing the leakage inductance responsible for the ringing phenomenon.

The contradictory requirements of the variable frequency and variable input voltage at the fixed number of primary turns make the transformer design complex. Instead, fixing of the input voltage allows for a wide frequency tuning range, meaning that the procedure can be simplified. The formula for calculating the number of primary turns is given by

$$N_p = \frac{V_{in} \times 10^4}{4 \times A_e \times B_{\max} \times f}, \quad (1)$$

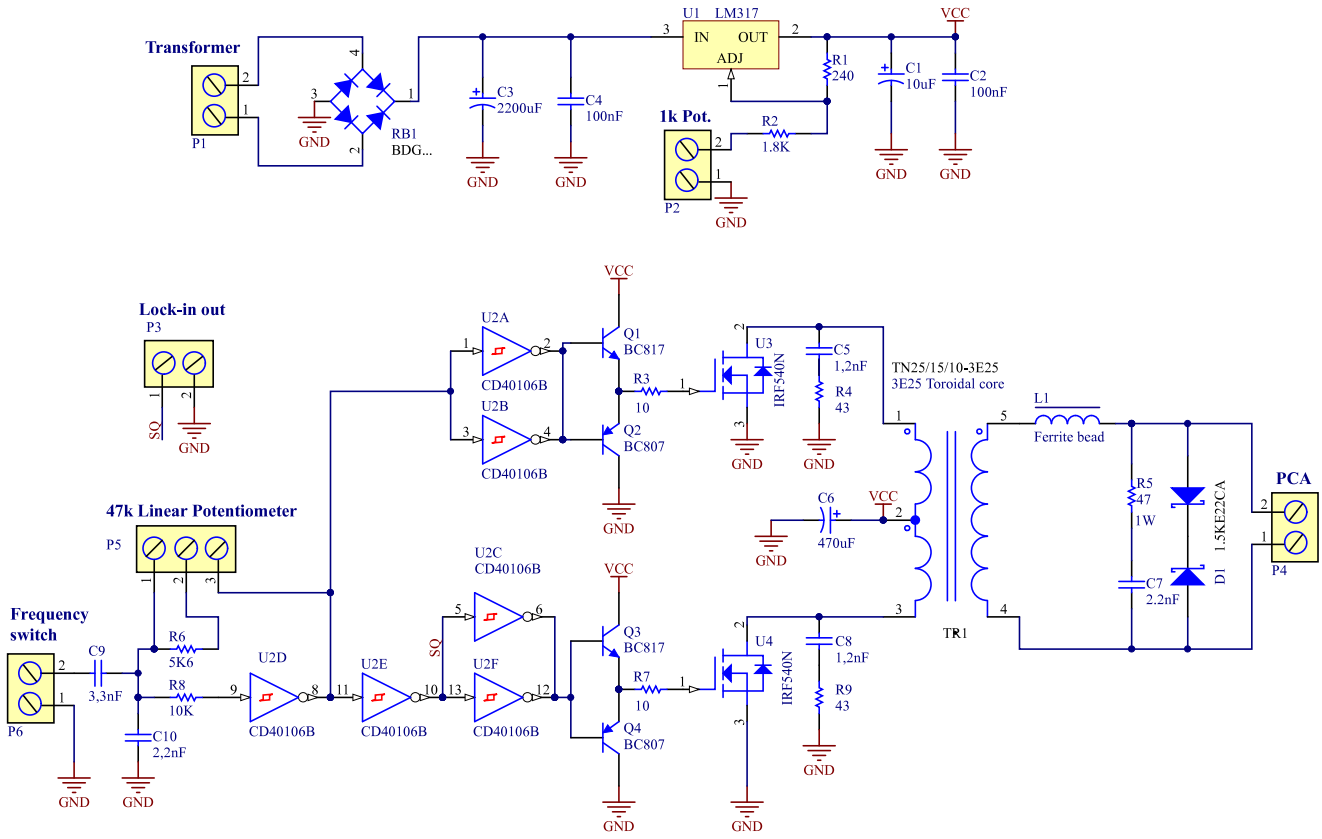

FIG. 3. Schematic diagram of the electronic chopper.

where V_{in} is an input voltage, f is an operating frequency, and A_e is the characteristic parameter of the core—an effective core area in square centimeters. The minimal switching frequency f should not be in the audible range; hence, 30 kHz was chosen as a lower limit. It can be seen from formula (1) that the higher the frequency is, the lower the number of turns that are needed is. However, as the frequency increases, switching losses increase too. Winding more turns than is optimal however results in a raised power dissipation. The calculated number of 12 turns per winding at an input voltage of 10 V and at the minimal operating frequency of 30 kHz enabled operation up to maximum of 200 kHz.

The maximum magnetic flux B_{max} has been assumed in the calculations to be lower than 150 mT. Due to the deterioration in performance caused by the temperature- and frequency-dependent effects, this ensured that the core was not saturated and provided a margin of safety. Twelve turns in the primary circuit correspond to the 140 mT of the magnetic flux in the core which met the requirements.

The skin-effect in copper wires causes current to flow near the external surface. The minimal wire diameter for a copper conductor, where the current density falls to $1/e$, is

$$d = 2 \times \frac{1}{\sqrt{\mu_0 \times \pi \times \sigma \times f}} \approx \frac{2 \times 6.6 \times 10^{-2}}{\sqrt{f}}, \qquad (2)$$

where f denotes the frequency and σ is the specific conductance of copper. The required wire diameter, for a frequency of 30 kHz, is about 0.7 mm. Wire of such a diameter was thus used for the winding of the step-up transformer.

C. Generator

The CMOS Schmitt trigger is the main and only active component in a square waveform generator. Due to alternating the charging of the capacitor through a resistor, the 50% duty square wave is generated. The generation frequency can be set by changing the value of the capacitor or feedback resistor and is given by $1/(1.2 \times R \times C)$. The frequency stability is sufficient to perform the measurements with a lock-in amplifier.

IV. MEASUREMENTS

The circuit was analyzed for any possible misbehavior, i.e., overstepping of the set amplitude, frequency instability, and possible high-noise levels. It is crucial to protect an expensive and sensitive photoconductive antenna from voltage spikes, breakdown voltage,[20] or, possibly, electrostatic discharge. The last two are eliminated by the configuration of the isolating transformer, along with protecting diodes. In the event of a rapid change of voltage (not caused by the circuit itself), the secondary coil acts as a short circuit, preventing any damage. Measurements taken with an oscilloscope are shown in Fig. 4. The voltage overshoots are 1.6 V (~7.0%) and 2.0 V (~8.7%), for a chopping frequency of 32 kHz and 200 kHz, respectively.

The FFT analysis (RBW = 5 Hz, span 25 kHz) presented in Fig. 5 shows excellent SNR performance of more than 100 dB with respect to the center frequency component. The amplitude of the first sinusoidal term of the Fourier

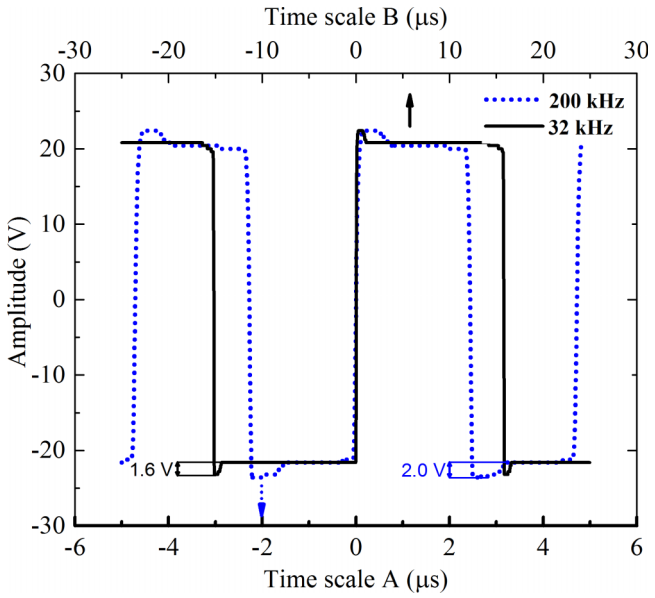

FIG. 4. Time waveform taken with an oscilloscope. Trigger set at 0 μs.

expansion calculated for the square wave of amplitude A equals $4A/\pi$. In the presented device, for the modulation amplitude $A = 20$ V, the measured amplitude V_1 of the dominant frequency component was 25.57 V_{peak}—negligibly different from the theoretical value (0.11 V, which is ~0.4% of the relative error). The spurious-free dynamic range (i.e., the difference between the fundamental component and the strongest distortion product in the spectrum, in dB scale) in the measured frequency region exceeded 30 dBc. The chopper therefore has little to no impact on the noise performance of the system.

An ideal oscillator would produce a single-line spectrum with a Dirac-delta-like shape, whereas the time-domain instabilities of the oscillator broaden the spectrum, thus producing the noise sidebands within a lock-in detection bandwidth. Spectrum of our electronic chopper has the shape of the aforementioned high-Q circuit, with possibility of

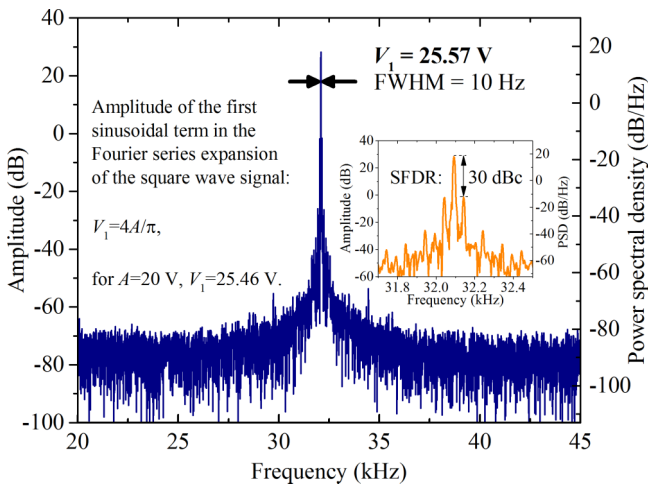

FIG. 5. Power spectrum and the power spectral density of the generated signal. In the frequency domain, the center frequency of 32.09 kHz is >100 dB higher than the noise floor in this spectral region.

further narrowing by means of the quartz clock generator usage. In contrast, optical choppers are known for introducing considerable rotation frequency fluctuations, which result in a low-Q reach in phase noise poor spectral characteristics.

For the sake of the noise analysis, we will briefly describe how the LIA picks up the noise in the experiment. The LIA measures signals close to the reference (chopping) frequency, far from the DC region, filtered by a low-pass digital filter, which is characterized by the slope and the time constant, τ. The noise power—a product of noise power spectral density and the bandwidth—can be minimized by narrowing the detection window. Mathematically, the RMS noise power coupled at a given equivalent noise bandwidth (ENBW) of the filter and the time constant τ is expressed as

$$P_{noiseRMS} \propto V^2_{noiseRMS} \propto ENBW \propto \frac{1}{\tau}. \quad (3)$$

For a two-stage filter (12 dB/octave) embedded in the LIA, the ENBW is 125 Hz for τ = 1 ms and 78.125 Hz in the case of a four-stage filter (24 dB/octave). Increasing the time constant τ minimizes the noise power, although one must wait longer for the chopped signal voltage to reach the final value because the filter acts here like a near-DC stimulated RC circuit. Since in the time-domain measurement the optical delay line moves at a constant speed, the high time constant may result in over-smoothing of the terahertz trace. *Per contra* the low value of τ introduces more noise. Consequently, the optimal choice of the lock-in time constant τ and the delay line scanning speed ν is crucial. In commercially available spectrometers, the high value of the signal-to-noise ratio of the time-domain signal is achieved either by the thousands of fast scans with a low integration time constant or by a single point-by-point slow scan with an integration time of 100 ms or more. In the first case, scans are captured and then averaged with the underlying assumption of the uncorrelated Gaussian noise. However, if the positioning of the linear stage is not repeatable, broadening of the pulse and limiting of the spectral coverage will be observed. In the second case, slow scans are, however accurate, the time of measurement grows notably. Thus, the first approach seems to be considered technically reasonable and is widely used in commercially available spectrometers.

To determine the performance and characteristics of the built device, the terahertz time-domain data were acquired. We concerned ourselves with the influence of the electronic chopper on the detected THz pulses. In the aspect of the laser noise characteristics,[6] it is a key point in determining an optimal modulation frequency. For different modulation frequencies, the device's own noise level was approximately the same; thus, the overall SNR is affected by other unknown factors, such as environmental electromagnetic noise and power line hum. The upper frequency of the measurements was limited by the maximum reference frequency of the SR830 (Stanford Research Systems) lock-in amplifier. This abnormal effect is shown in Table I.

We captured the temporal profiles of the THz signals at three different integration time constants (300 μs, 1 ms, and 3 ms), ensuring the absence of any influence of the parameters of the homodyne measurement technique on the obtained noise characteristics versus frequency. The scanning speed,

TABLE I. Measured signal-to-noise ratio over chopping frequency for 1 ms lock-in integration time constant.

F (kHz)	SNR (dB)	F (kHz)	SNR (dB)
35	44.7	70	34.0
40	44.9	75	38.5
45	36.9	80	24.5
50	37.8	85	45.1
55	44.5	90	32.2
60	24.1	95	31.0
65	8.3	100	45.2

ν, of the optical delay line in the optical chopper experiment corresponds to the 20 ps of the terahertz time-domain trace acquired within 1 s time, while for the electronic chopper speed was 200 ps/s, as such was the limiting value for our motorized linear stage. The scanning speed discrepancy, here ten-to-one, was caused by an extremely noisy terahertz signal in the optical chopper scheme at higher acquisition rates.

The captured profiles and the corresponding spectra are illustrated in Figs. 6(a)-6(c). The corresponding SNR has been measured by taking a window for the first 25 ps of the pulse to estimate the noise power, but estimating the power of the signal from the subsequent time period.

The time-domain signals were normalized prior to calculation of the Fourier transform; however, the amplitude of the optically chopped terahertz signal was approximately 50% lower than for the electronic chopping scheme. Our observation is consistent with previous studies on the terahertz photoconductive antenna chopping schemes.[7] In Fig. 6(a), the time-domain signals acquired using the electronic and optical chopper are shown with the chopping frequencies of 100 kHz and 1 kHz, respectively. The integration time was set to 1 ms. Despite the lower acquisition speed, the signal corresponding to the optical chopping scheme (blue/gray) is rich in the high frequency noise. The inset shows the main terahertz pulse zoomed. The high frequency noise of the optical chopper (blue/gray) elevates the spectrum in the frequencies above 1 THz in this way lowering the SNR performance. The electronic chopper (black) provides, on the contrary, a smooth and clean trace. In favor of noise reduction, the time constant can be increased. This strategy is illustrated in Fig. 6(b)—measurements were taken with a 3 ms integration time. As expected, the SNR factor for the optical chopper has risen. Regrettably, the terahertz pulse in the electronic chopping scheme in this case is over-smoothed and stretched in time, resulting in the narrowed spectrum. The signal-to-noise performance of the electronic chopper drops by 2.2 dB compared to the previous acquisition scenario. The over-smoothing problem can be easily overcome by a slight reduction of the scanning speed. The voltage in the lock-in filters would reach the final value of the DC signal at a given delay line position.

Superiority of our device over the optical chopper in a low time constant (300 μs) measurement is additionally demonstrated in Fig. 6(c). The SNR of the optical chopper reaches the unacceptable value of 2.9 dB—the signal is intensively perturbed by the high frequency noise. Notably,

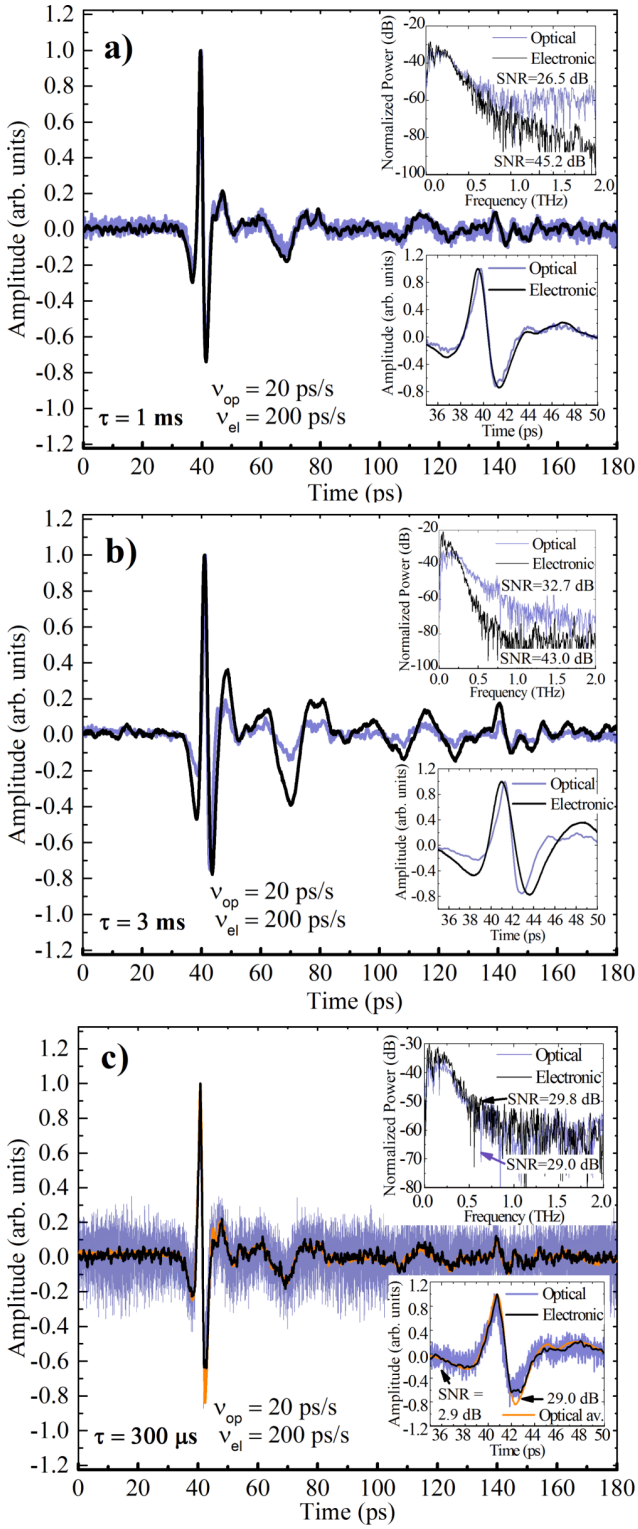

FIG. 6. Terahertz time domain signals. Electronic chopper at 100 kHz chopping frequency (black thin line) and the optical chopper at 1 kHz (blue/gray line). Insets show calculated FFT with the estimated SNR and zoom on the main THz pulse. The scanning speed for the optical chopper was one order of magnitude lower than for the electronic one. (a) Shows plots for the 1 ms integration time constant of the lock-in, (b) τ = 3 ms, and (c) τ = 300 μs with added averaged trace of optical chopper (orange, the smoothest).

the moving average filtered trace (orange) follows the electronic chopper-based signal (without processing) with good agreement. The calculated SNR of the averaged trace is 29.0 dB, but the moving average filter always introduces

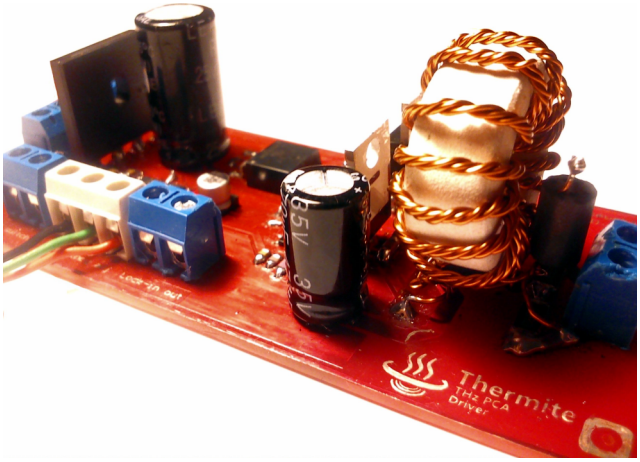

FIG. 7. Photograph of the built device.

a degree of freedom to signal preprocessing, changing the resulting spectrum. Conversely, in the electronic chopper-based detection scheme, the SNR of the raw terahertz time domain trace is tolerable—29.8 dB. In the inset figure, one can see that the high frequency noise in the two chopping schemes does not perturb the spectrum shape completely. However, in demanding spectroscopic experiments, the choice of the maximum allowable integration time for rejecting the noise is preferred.

V. CONCLUSION

The proposed electronic device outperforms the mechanical chopper, by eliminating unwanted vibrations and acoustic noise in the measurement system. The bipolar driving scheme in its principle provides an extra 3 dB of SNR in comparison to mechanical chopping. We show that the proposed chopping scheme enables to increase of the scanning speed and improves the noise performance in the terahertz spectroscopic experiments at low integration time constants, whereas the performance of the optical chopper is even worse. The wide tuning range of the modulation frequency provides an opportunity to suppress environmental noise (independent of the noise of the laser and the electronics). This is the only way to maintain the critical Nyquist–Shannon sampling frequency, when a high sampling rate is necessary.

Due to the simplicity of our design, it can easily be built by a person with a modest knowledge of electronics. Widely available components, and an easy-to-wind transformer, make the presented solution cost-efficient. It is worth mentioning that the power efficiency of the equipment is very attractive in comparison to usage of a standalone generator and amplifier.

The full galvanic isolation provided by the transformer breaks the ground loop, if present, reduces the noise and limits the number of connecting wires. The rise time of 90 ns for the full output voltage swing for the given frequency tuning range ensures a sharp square wave with a low settling time. The shorter rise time value corresponds to the larger voltage oscillations. To damp them more efficiently, the MOSFET gate resistor's value should be increased. It smoothens the voltage transitions but increases the power dissipation. If higher frequency stability is desired, the CMOS Schmitt RC generator can be replaced with a quartz-based oscillator. The power stage, however, remains the same.

The application of the device is not limited to terahertz instrumentation. Other applications are possible: for instance, it can also be used for biasing a large piezoelectric transducer. A working device is presented in Fig. 7.

ACKNOWLEDGMENTS

We would like to thank Dr. Martin Mikulics from Peter Grünberg Institut, Germany, for providing the samples of photoconductive antennas. This work was supported by an internal university Grant No. S50037/W4K3.

[1]S. Verghese, K. McIntosh, and E. Brown, "Optical and terahertz power limits in the low-temperature-grown GaAs photomixers," Appl. Phys. Lett. **71**(19), 2743–2745 (1997).
[2]S. Verghese, K. McIntosh, and E. Brown, "Highly tunable fiber-coupled photomixers with coherent terahertz output power," IEEE Trans. Microwave Theory Tech. **45**(8), 1301–1309 (1997).
[3]P. U. Jepsen, R. H. Jacobsen, and S. Keiding, "Generation and detection of terahertz pulses from biased semiconductor antennas," J. Opt. Soc. Am. B **13**(11), 2424–2436 (1996).
[4]D. H. Auston, "Electro-optic generation and detection of femtosecond electromagnetic pulses: DTIC document," Technical Report, Final rept. 1 Aug 88-30 Sep 91 Accession Number: ADA244276, 1991.
[5]D. Mittleman *et al.*, *Sensing with Terahertz Radiation* (Springer Berlin, 2003), Vol. 337.
[6]T. Yasui and T. Araki, "Dependence of terahertz electric fields on electric bias and modulation frequency in pulsed terahertz emissions from electrically-modulated photoconductive antenna detected with free-space electro-optic sampling," Jpn. J. Appl. Phys., Part 1 **44**(4R), 1777 (2005).
[7]R. Yano, T. Hattori, and H. Shinojima, "Bias field modulation of photoconductive antenna for emission and detection of terahertz electromagnetic waves," in *International Quantum Electronics Conference, 2005* (IEEE, 2005), pp. 1342–1343.
[8]L. Schmidt, S. Biber, G. Rehm, and K. Huber, "THz measurement technologies and applications," in paper presented at 14th International Conference on Microwaves, Radar and Wireless Communications, 2002, MIKON-2002, 2002.
[9]P. H. Siegel *et al.*, "Terahertz technology," IEEE Trans. Microwave Theory Tech. **50**(3), 910–928 (2002).
[10]Batop optoelectronics Instruction manual and data sheet PCA-40-05-10-800-x.
[11]K. Ezdi, B. Heinen, C. Jordens *et al.*, "A hybrid time-domain model for pulsed terahertz dipole antennas," J. Eur. Opt. Soc. **4**, 09001 (2009).
[12]X. C. Zhang and J. Xu, *Introduction to THz Wave Photonics* (Springer, 2010).
[13]R. Yano, T. Hattori, and H. Shinojima, "Improvement of signal-to-noise ratio of terahertz electromagnetic waves by bias field modulation of photoconductive antenna," Jpn. J. Appl. Phys., Part 1 **45**(11R), 8714 (2006).
[14]T. Usher and G. A. McAuley, "High-voltage MOSFET bipolar square-wave generator," Rev. Sci. Instrum. **64**(7), 2027–2030 (1993).
[15]B. Schulkin, "Miniature terahertz time-domain spectrometry," Ph.D. dissertation (Rensselaer Polytechnic Institute, 2008).
[16]W. Andreycak, Practical Considerations In High Performance MOSFET, IGBT and MCT Gate Drive Circuits, Unitrode Corporation, Application Note U-137, 2001.
[17]Maxim Integrated, Application Note 3835-CCFL Push-Pull Snubber Circuit, 2006, see https://www.maximintegrated.com/en/app-notes/index.mvp/id/3835.
[18]F. Xw, L. Xw, and T. Zq, "Nanosecond square high voltage pulse generator for electro-optic switch," Rev. Sci. Instrum. **82**(7), 075102 (2011).
[19]Colonel Wm. T. McLyman, *Designing a 100 kHz 32 watt Push-Pull Converter* (2002).
[20]A. Singh, S. Pal, H. Surdi, S. Prabhu, V. Nanal, and R. Pillay, "Highly efficient and electrically robust carbon irradiated semi-insulating GaAs based photoconductive terahertz emitters," Appl. Phys. Lett. **104**(6), 063501 (2014).